Electronic Supplementary Material (ESI) for Physical Chemistry Chemical Physics.

Electronic Supporting Information

2-Chloromalonaldehyde, a Model System of Resonance-Assisted Hydrogen Bonding: Vibrational Investigation

Alejandro Gutiérrez-Quintanilla[a,b], Michèle Chevalier[a*], Rasa Platakyte[a,c], Justinas Ceponkus[c], German A. Rojas-Lorenzo[b], Claudine Crépin[a]

[a] Institut des Sciences Moléculaires d'Orsay (ISMO), UMR 8214, CNRS, Univ. Paris- Sud, Université Paris-Saclay UMR 8214, F-91405 Orsay, France

[b] Instituto Superior de Tecnologías y Ciencias Aplicadas (InSTEC), Universidad de La Habana. Ave. Salvador Allende No. 1110, Quinta de los Molinos, La Habana 10400, Cuba.

[c] Department of General Physics and Spectroscopy, Vilnius University, Sauletekio av. 9 bat. III, L-10222 Vilnius, Lithuania

**michele.chevalier@u-psud.fr*

Table of Contents:

I. Theoretical calculations

Geometry optimizations were performed for all isomers (dialdehyde and eight enol forms) of 2-chloromalonaldehyde, followed by frequency calculations. In all the steps we used DFT level of theory with M06-2X functional[1] and 6-311++G(3df,3pd) basis set, using Gaussian 09 (revision A 02) software.[2] The choice of the M06-2X functional was based on the good performance of this functional to describe medium range interactions, which can be very important in these systems.[3] A very tight convergence criteria and a superfine optimization grid (-96032

code in Gaussian 09 meaning 96 radial points and a spherical product grid of 32 x 64 angular points per shell) was also used. The option “internal” was checked to give an idea of the decomposition of the modes. Vibrational frequencies were obtained by means of harmonic and anharmonic approaches. It allows calculations of Zero-Point Energies (ZPE) for all the structures. For the presented harmonic spectra, a scaling factor of 0.968 was used. This value was optimized to fit the theoretical results to the experimental values. It takes into account the average anharmonicity but reflects also the interaction between the host and the molecule. The same scaling factor was used for the different matrices. In comparison with experiments, no improvement was obtained when using anharmonic frequencies compared to the harmonic scaled ones. Only the latter are presented in the tables. The same calculations were applied to malonaldehyde in order to compare theoretical results of MA and 2-ClMA.
All these calculations were run in the GMPCS cluster (Grappe Massivement Parallèle de Calcul Scientifique) at Orsay, Université de Paris-Saclay.

Molecular dynamics simulations were carried out in order to describe the different trapping sites occupied by MA and 2-ClMA in Ne and Ar matrices. The method simulates the deposition process in order to get the most stable sites, formed during the rare gas (Ne, Ar) crystal growth. The model used was successfully applied before by other groups and was described in Ref.4 . The interatomic interactions were described by Lennard Jones pair potentials, while intramolecular interactions by CFF force fields for bonding potentials, planar angle potentials and dihedral angle potentials.[5,6] In the model four shell atoms lying in 100 crystallographic plane ordered along z axis were considered as a framework to build the fcc crystal. Each shell contains 72 rare gas atoms. Periodic boundary conditions were applied in *x* and *y* directions to simulate an infinite surface. In the case of Ne crystals growth, thermal anhamornic quantum corrections were applied at the effective temperature of 17 K.[7] The systems in Ar were thermalized at an effective temperature of 49K in order to consider the ZPE in the classical approach used for describing the real process at 7K.[8] The molecule and 576 rare gas atoms covering 12 rare gas shells were falling down on the equilibrated surface, with randomly distributed initial *(x,y)* positions. The time between 2 consecutive impacts was 5 ps. The growth process was repeated 100 times to achieve the statistics.

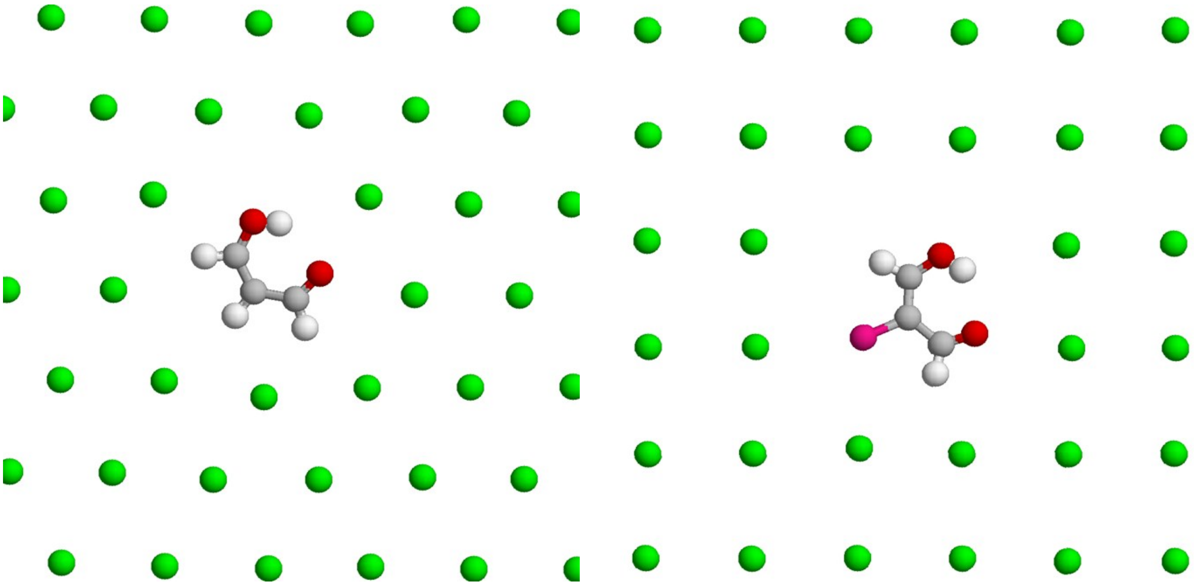

Figure S1: Typical trapping sites of MA (left panel) and 2-ClMA (right panel) in Ar obtained in classical dynamics calculations; only the layer occupied by the molecule is shown. MA takes the place of three Ar atoms of the lattice. The molecule which was initially aligned parallel to the 100 plane moves and reaches a new alignment along the 111 crystallographic plane. The 2-ClMA molecule occupies a four Ar atoms vacancy site and remains aligned along 100 plane. Simulations with the initial surface aligned along 111 planes were carried out and the results were similar.

II. Experimental setups

Two different matrix isolation experimental setups were used for IR studies: one for neon (Messer 5.0) and argon (Messer 5.0) matrices (previously described in reference 9) and the other for *para*-hydrogen (pH_2) matrix. When using the first setup, Ne and Ar were deposited at 7 K and 20 K respectively. The reservoir containing 2-ClMA was attached to the deposition tube, in front of the entrance in the cryostat. The latter included two closed cycle helium cryostats: one for the *ortho/para*-hydrogen conversion process (Air Products, Displex DE202), using Fe_2O_3 powder (Sigma-Aldrich 99 %) as catalyst, and the other for the sample deposition (ICE: Innovative Cryogenic Engineering, RDK 415D, He Compressor: Sumitomo F-50). Both cryostats were connected using a stainless steel tube (1 m long). In the cryostat devoted to *ortho/para*- conversion, the temperature was raised to 18 K after conversion around 15 K, and the pH_2 was transferred to the deposition cryostat via the stainless steel tube. A small reservoir containing the solid sample of 2-ClMA was attached to this tube. Two Swagelok microvalves allowed controlling the host gas flux (pH_2) and the amount of 2-ClMA vapor from the sample. The mixture of gases arrived directly in front of the internal diamond window (2.8 K) fixed to the cold head of the other cryostat. The cold head could rotate around its axis after gas deposition to record the IR spectrum of the sample. This cryostat was pumped by a turbomolecular pump (Oerlikon, Leybold vacuum, Turbovac 600C, pumping speed for H_2: 570 $l.s^{-1}$), which allowed reaching pressures below 10^{-6} mbar at 293 K. The pump was directly attached to the vacuum chamber of the cryostat to get a better pumping efficiency. The pH_2 converter was pumped by a diffusion pump (CIT Alcatel). The IR spectra were obtained using a FT-IR spectrometer (Nicolet 670/870) at a resolution of 0.5 cm^{-1}.

For Raman spectra in argon (Messer 5.0) matrix, the samples were deposited on an aluminum plate cooled down to 9 K in a closed cycle helium cryostat (Leybold Hareus RW2). They were excited with a diode laser at 785 nm. Spectra were recorded with a Raman FT (MultiramII Bruker) with a resolution of 2 cm^{-1} .

2-ClMA (Acros, 95%) was always used as supplied from the manufacturer, without further purification process. The low vapor pressure of this molecule is entrained by the host gas flow. The guest/host ratio was not well defined in this experimental method of deposition but IR spectra showed well isolated molecules and allowed 1/1000 estimated 2-ClMA/host ratios. In Raman experiments, this ratio was always over 1/100 and 1/200. Concentration was higher than in IR experiments to enhance the small scattering signal for Raman spectra and was obtained by heating the 2-ClMA reservoir around 80°C.

III. Table S1

IR band positions (cm-1) of CCC in Ne, pH2 and Ar matrices, compared with scaled harmonic calculated wavenumbers (scaling factor of 0.968). Site structures reported as value1|value2. Theoretical wavenumbers (cm-1), IR intensities (km/mol) and Raman activities (Å4/amu) are reported for all the modes. Values in italic correspond to bands recorded in the Raman spectrum.

Experimental			Calculations				
Ne	pH_2	Ar	Mode description[a]	CCC			
IR	IR	IR/Raman		$\tilde{v}$, cm^{-1}			
				Harm	Anharm	IR int	Ram. act.
			νOH	3280.8	2852.1	208	24
2917	2909.8	2910	νC_3H	3112.0	2991.2	8	82
2875.1	2876.7	2885.8/*2883*	νC_1H	2945.5	2767.4	40	96
1670.2	1665.8	1664.7/*1665*	($\nu C=O + \nu C=C$) (oph)	1716.6	1743.7	175	13
1587-1575	1608.8 1563.0	1601.5/*1598* 1579.3/*1575*	δOH+ ($\nu C=O + \nu C=C$) (iph)	1584.9	1585.0	303	62
1396.2	1397.0	1396.2	($\delta C_1H + 3\delta C_3H$) (iph)	1392.1	1420.8	28	1
1347.7	1346.9		($\delta C_1H + \delta C_3H$) (oph)	1342.1	1364.9	31	9
1343.0	1344.7 1317	1343.4/*1344* 1314/*1317*	δOH	1339.2	1330.5	110	24

1233.6	1232.3	1229.0	δOH + δC$_3$H	1235.1	1265.5	236	0.1
1070.6	1076.4 1068.1	1070/*1068* 1066.1/*1068*	νC-C + δCCC + νC-Cl	1070.8	1099.0	83	6
	1016	1013|1010	(γC$_1$H + γC$_3$H) (oph)	1016.9	1040.1	4	0.4
953.7	952.8	952.7 950.8	(γC$_1$H + γC$_3$H) (iph)	969.4	980.6	17	1
916.5	922.5 914.7	918 913.1/*914*	Δ	897.8	927.9	44	12
830.8	829.3	823.5	γOH	837.4	819.2	87	1
		505	Δ	500.6	521.7	16	5
		474	Δ + νC-Cl	470.7	486.4	6	7
			γC$_3$H	368.8	373.7	2	1
			γC$_1$H	281.9	293.1	2	1
		278	δCCl	277.9	285.2	4	3
			Δ (νO···H)	232.9	284.8	7	0.4
		225	γC$_1$H	212.3	221.0	6	1

[a]ν- stretching, δ-in plane bending, γ-out of plane bending, Δ-in plane ring deformation, (oph) out of phase, (iph) in phase, labelling of carbon atoms from Figure 1.

References:

1 Y. Zhao and D. G. Truhlar, The M06 suite of density functionals for main group thermochemistry, thermochemical kinetics, noncovalent interactions, excited states, and transition elements: Two new functionals and systematic testing of four M06-class functionals and 12 other function, *Theor. Chem. Acc.*, 2008, **120**, 215–241.

2 M. J. Frisch, G. W. Trucks, H. B. Schlegel, G. E. Scuseria, M. A. Robb, J. R. Cheeseman, G. Scalmani, V. Barone, B. Mennucci, G. A. Petersson, H. Nakatsuji, M. Caricato, X. Li, H. H. P., A. F. Izmaylov, J. Bloino, G. Zheng, D. J. Sonnenb, M. Hada, M. Ehara, K. Toyota, R. Fukuda, J. Hasegawa, M. Ishida, T. Nakajima, Y. Honda, O. Kitao, H. Nakai, T. Vreven, J. Montgomery, J. A., J. E. Peralta, F. Ogliaro, M. Bearpark, J. J. Heyd, E. Brothers, K. N. Kudin, V. N. Staroverov, R. Kobayashi, J. Normand, K. Raghavachari, A. Rendell, J. C. Burant, S. S. Iyengar, J. Tomasi, M. Cossi, N. Rega, J. M. Millam, M. Klene, J. E. Knox, J. B. Cross, V. Bakken, C. Adamo, J. Jaramillo, R. Gomperts, R. E. Stratmann, O. Yazyev, A. J. Austin, R. Cammi, C. Pomelli, J. W. Ochterski, R. L. Martin, K. Morokuma, V. G. Zakrzewski, G. A. Voth, P. Salvador, J. J. Dannenberg, S. Dapprich, A. D. Daniels, O. Farkas, J. B. Foresman, J. V. Ortiz, J. Cioslowski, D. J. Fox, R. D. 0. Gaussian 09, M. J. Frisch, G. W. Trucks, H. B. Schlegel, G. E. Scuseria, M. A. Robb, J. R. Cheeseman, G. Scalmani, V. Barone, B. Mennucci, G. A. Petersson, H. Nakatsuji, M. Caricato, X. Li, H. H. P., A. F. Izmaylov, J. Bloino, G. Zheng, D. J. Sonnenb, M. Hada, M. Ehara, K. Toyota, R. Fukuda, J. Hasegawa, M. Ishida, T. Nakajima, Y. Honda, O. Kitao, H. Nakai, T. Vreven, J. Montgomery, J. A., J. E. Peralta, F. Ogliaro, M. Bearpark, J. J. Heyd, E. Brothers, K. N. Kudin, V. N. Staroverov, R. Kobayashi, J. Normand, K. Raghavachari, A. Rendell, J. C. Burant, S. S. Iyengar, J. Tomasi, M. Cossi, N. Rega, J. M. Millam, M. Klene, J. E. Knox, J. B. Cross, V. Bakken, C. Adamo, J. Jaramillo, R. Gomperts, R. E. Stratmann, O. Yazyev, A. J. Austin, R. Cammi, C. Pomelli, J. W. Ochterski, R. L. Martin, K. Morokuma, V. G. Zakrzewski, G. A. Voth, P. Salvador, J. J. Dannenberg, S. Dapprich, A. D. Daniels, O. Farkas, J. B. Foresman, J. V. Ortiz, J. Cioslowski, D. J. Fox and 2009. Gaussian, Inc., Wallingford CT, 2009.

3 Y. Zhao and D. G. Truhlar, Applications and validations of the Minnesota density functionals, *Chem. Phys. Lett.*, 2011, **502**, 1–13.

4 C. Crépin, P. de Pujo, B. Bouvier, V. Brenner, P. Millié, C. Crepin and P. Millie, A simulation of

naphthalene matrix isolation: comparison with experiments, *Chem. Phys.*, 2001, **272**, 243–258.

5 J. R. Maple, M.-J. Hwang, T. P. Stockfisch, U. Dinur, M. Waldman, C. S. Ewig and A. T. Hagler, Derivation of class II force fields. I. Methodology and quantum force field for the alkyl functional group and alkane molecules, *J. Comput. Chem.*, 1994, **15**, 162–182.

6 H. Sun, S. J. Mumby, J. R. Maple and A. T. Hagler, An ab Initio CFF93 All-Atom Force Field for Polycarbonates, *J. Am. Chem. Soc.*, 1994, **116**, 2978–2987.

7 L. Uranga-Pina, A. Martinez-Mesa, J. Rubayo-Soneira and G. Rojas-Lorenzo, An effective temperature approach for molecular dynamics simulations of quantum solids, *Chem. Phys. Lett.*, 2006, **429**, 450–456.

8 J. P. Bergsma, P. H. Berens, K. R. Wilson, D. R. Fredkin and E. J. Heller, Electronic-Spectra from Molecular-Dynamics - a Simple Approach, *J. Phys. Chem.*, 1984, **88**, 612–619.

9 A. Gutierrez-Quintanilla, M. Chevalier and C. Crepin, Double deuterated acetylacetone in neon matrices: infrared spectroscopy{,} photoreactivity and the tunneling process, *Phys. Chem. Chem. Phys.*, 2016, **18**, 20713–20725.